THERMAL DESIGN ASPECTS OF GAS-COOLED POWER REACTOR CORES

M. Troost, General Atomic, San Diego, California
P. Fortescue, General Atomic, San Diego, California
R. N. Lyon, Oak Ridge National Laboratory, Oak Ridge, Tennessee
G. Melese, General Atomic, San Diego, California
G. Samuels, Oak Ridge National Laboratory, Oak Ridge, Tennessee,

1. Introduction

Before considering in detail thermal designs of selected reactor cores, it is desirable to look at the picture somewhat more broadly, in order to understand the principles responsible for the wide design diversities exhibited by the many variants of the gas-cooled reactor. Considerable insight into the general characteristics of gas cooling as applied to reactors is forthcoming at once from the most elementary arguments. For simplification, only perfect, constant-property gases and smooth uniform passages are used. Acceleration of the gas is neglected and a uniform flow distribution is assumed. Temperature drops inside fuel elements are not included. Some useful relations between reactor parameters are now derived.

The following basic relations are used:

Frictional pressure drop	$\Delta p = 2fLV^2\rho/(Dg_c)$	(1)
Mass balance	$w = \rho \epsilon SV$	(2)
Heat balance	$Q = wc_p\Delta T$	(3)
Heat transfer	$\Delta t = Q/(\rho V c_p\ FAN_{St})$	(4)
Pumping power in the core	$W = (w\Delta p/\rho)\ [T_0/(T_0 + \Delta T/2)]$	(5)
Reynolds analogy	$N_{St} = \alpha f$ (for smooth surfaces and $N_{Pr} = 1, \alpha = 1/2.$)	(6)
Hydraulic diameter	$D = 4\epsilon SL/A$	(7)
Specific heat	$c_p = C_p/M$	(8)
Average density	$\rho = pM/[R(T_0 + \Delta T/2)].$	(9)

Here, Δp = Core pressure drop
V = Average gas velocity
L = Core length
D = Hydraulic diameter of channel
ρ = Average coolant density
w = Total mass flow

DISCLAIMER

g_c = Conversion factor (32.2 ft × pounds mass/(sec^2 × pounds force)

ϵ = Void fraction

ΔT = Coolant temperature rise in the core

Δt = Average surface to coolant temperature drop

N_{St} = Stanton number ($h/V\rho c_p$)

W = Pumping power in the core

N_{Pr} = Prandtl number ($c_p\mu/k$)

C_p = Coolant molar heat capacity

p = Average ambient pressure

N_{Re} = Reynolds number ($DV\rho/\mu$)

f = Friction factor

S = Frontal area of core

c_p = Coolant specific heat capacity

Q = Total thermal output

F = Heated fraction of the channel surface

A = Total frictional area in the core

h = Heat transfer coefficient

T_o = Absolute inlet temperature

μ = Absolute viscosity

k = Thermal conductivity

M = Molecular weight

R = Universal gas constant

Appropriate manipulation yields a general relation between thermal output per unit frontal area of the core Q/S as a function of the allowable core pumping fraction W/Q, the void fraction ϵ and $\Delta t/\Delta T$, without any knowledge of the detailed core structure

$$Q/S = \frac{\epsilon p \Delta T}{RT_o}\left(\frac{C_p^3}{M}\frac{W}{Q}\frac{F\,\Delta t 2\alpha g_c}{1 + \Delta T/2T_o}\right)^{\frac{1}{2}} . \qquad (10)$$

The required heated surface per unit frontal area of the core is

$$FA/S = \epsilon\,\Delta T/(N_{St}\,\Delta t), \qquad (11)$$

and the required hydraulic diameter of a channel is

$$D = 4LN_{St}F\,\Delta t/\Delta T . \qquad (12)$$

Using the friction factor correlation for turbulent flow in smooth tubes

$$f = 0.046\,N_{Re}^{-0.2} , \qquad (13)$$

we find an expression for the hydraulic diameter,

$$D = 0.136\,(2\alpha LF\,\Delta t/\Delta T)^{0.835}\,[S\epsilon C_p\mu\Delta T/(QM)]^{0.166} . \qquad (14)$$

The term $(C_p^3/M)^{\frac{1}{2}}$ emerges as a criterion of usefulness of coolants (Eq. 10), but the required heated surface varies for different coolants (Eq. 14). The choice of coolant, however, is mainly determined by such factors as inertness, irradiation damage, and availability. Since gross output varies as rapidly as the square root of the pumping fraction, it often pays to devote a substantial fraction of the reactor output to pumping. The gross output is found to be proportional to the gas pressure and independent of the core length.

The ratio of the heated surface to flow area, $FA/\epsilon S$, depends only on the Stanton number for a given temperature limitation (Eq. 11). For a fixed flow area, it is shown in Eq. 10 that the thermal output does not change if the friction factor and the Stanton number are increased by the same factor, i.e., α is constant but there is a corresponding reduction in the heated surface FA (Eq. 11). As shown in Section 6, we can use surface roughening that almost doubles the Stanton number for a penalty of locally tripling the friction factor. Since only the hotter 1/2 to 2/3 downstream section of the fuel element needs roughening, the over-all channel pressure drop is only doubled. When the surface temperature is limiting, the fuel-element diameter may thus be doubled and the number of fuel elements decreased by a factor of four, for a fixed total fuel-element volume, reactor size, total power and coolant temperatures; increased internal temperatures may now become a limiting factor.

2. Main Features of U.S. Gas-cooled Reactors

One type of gas-cooled reactor, e.g., EGCR (Experimental Gas Cooled Reactor) and EBOR (Experimental Beryllium Oxide Reactor), uses oxide fuel with metallic clad. These reactors are designed to take advantage of the high burnup potential of oxide fuel and the design freedom allowed by enrichment. The poor conductivity of the oxide, coupled with the desire for high power density, forces the use of groups of thin rods in channels. High surface temperatures necessitate the use of stainless steel or Hastelloy-X clads, whose low thermal conductivities render fins inefficient. By using roughened surfaces, the allowable surface heat flux may be increased. The corresponding higher fuel temperatures may be limited by using hollow fuel elements. Hot-spot temperatures are usually obtained by comparing the results of calculations with several assumptions on their causes, rather than by using multiplying factors.

In another type of gas-cooled reactor, e.g., HTGR's (High Temperature Gas Cooled Reactors) and pebble bed reactors, all-ceramic fuel elements are used. The elimination of metallic cladding allows very high surface temperatures. As the fuel is heavily diluted by moderator, structural fuel irradiation damage is virtually eliminated as a burnup-limiting factor. The incentive to seek high coolant temperatures, and accompanying high plant efficiency, goes far beyond the direct effect on fuel costs, for, in general, it implies increased useful output from a given reactor thermal power and hence reduced unit capital costs of that substantial part of the plant. As shown by Table I, the HTGR class of reactors is capable of very satisfactory core power density. By virtue of the high temperature differentials and good steam conditions available, the associated boilers and turbines

can also be very compact. HTGR-type designs optimized for large-scale power production have, in fact, exploited these features to the point where powers of the order of 500 MW(e) are contemplated from total plant containment volumes little larger than the 40-MW(e) Peach Bottom, for similar core power densities.

Some thermal design parameters of U.S. gas-cooled reactors under construction or in operation are presented in Table I. The corresponding fuel elements are shown in Fig. 1. Rocket and airplane reactors are not discussed, nor are fast gas-cooled reactors. EGCR and HTGR will be described in more detail in later sections. A common problem to all gas-cooled reactors is the possibility of a loss-of-coolant-flow accident. This is more serious for gas-cooled reactors than for liquid-cooled reactors because the afterheat cannot be absorbed by the coolant. U.S. gas-cooled reactors have therefore been equipped with internal heat sinks which absorb the heat of the initial transient resulting from temperature equalization within the fuel element which causes a rapid rise in surface temperature. Some kind of emergency cooling is supplied to remove the afterheat after the initial transient is over. Thus, the design power density of the reactor may be limited by afterheat-removal considerations.

EBOR, now under construction, is designed to test the high-temperature behavior of BeO as a reactor moderator.[1] The selection of the present EBOR fuel element was based, in part, on the inherent simplicity, the readily predictable thermal performance, and satisfactory behavior in the event of a loss-of-coolant accident. To achieve proper performance, the fuel rods must be closely spaced in the annular passage. The ratio of the minimum clearance between rods to the rod diameter is 0.14. The ratio of the pitch of the helical rod spacers to the rod diameter is 20. The coolant flow to each fuel element is orificed so that the maximum cladding temperature in each element is about the same. The local heat-transfer coefficient around a fuel pin may vary 20 to 30% about its average value.[2]

The 630-A reactor,[3] which is derived from the Aircraft Nuclear Propulsion program, is proposed as an integral nuclear steam generator for ship propulsion. In this reactor the thickness of the coaxial fuel rings within a fuel assembly is varied to give approximately equal heat fluxes from all rings. A re-entrant water-filled moderator tube is centered in each of the fuel tubes to reduce the flux depression through the assembly. The diameter of the moderator tube is varied in four radial zones in the reactor to obtain nearly the same surface heat flux for all radial positions. Heat losses to the water moderator have to be tolerated to ensure enough cooling by radiation if coolant flow is lost.

The ML-1 reactor[4] is a small portable unit using a closed-cycle gas turbine for power generation. The spacing of the stainless steel pressure tubes, which contain the fuel-element bundles, is varied to flatten the radial power distribution. The fuel loading of the pins within the bundle is varied to equalize the cladding temperatures. A 40-mil Hastelloy-X wire separates the pins from each other and from the inner liner that is itself insulated from the pressure tube by a 0.112-in. layer of Thermoflex (Al_2O_3-SiO_2).

The Ultra High Temperature Reactor Experiment (UHTREX)[5] is designed to supply process heat at very high temperatures. Since no cladding is used, the primary circuit contains large amounts of fission products.

3. EGCR Thermal Design

The fuel assembly for the EGCR consists of a seven-rod cluster of stainless steel tubes filled with cored, UO_2 pellets, each cluster supported within a 1-in.-thick graphite sleeve of 3-in. I.D. and 5-in. O.D. (see Fig. 1). There are six stacked fuel assemblies in each coolant channel.[6]

As unsymmetrical temperature variations around the rods result in differential expansion and bowing, initial emphasis was placed on minimizing the circumferential temperature variations in the six outer rods of the seven-rod cluster by proper radial location in the coolant channel. Since the rods are supported at the ends, such bowing restricts gas passage along the hotter portion of the rod, and results in further bowing. It is important to design the fuel assembly so that the total bowing and flow restriction does not result in a local rod-surface temperature that will damage the stainless steel fuel-rod tubes. To determine the temperature structure within a cluster, a rather extensive series of heat-transfer and fluid-flow experiments was conducted.[7,8] The most convenient qualitative experimental method was found to be measurement of the local removal of a naphthalene coating on one of the outer cluster tubes in an isothermal test using air.[9] Naphthalene removal is most uniform when the outer rods are equidistant between the center rod and the channel wall. However, heat-transfer tests indicate that the axial temperature rise of the gas is not uniform, and mixing between the passages of the cluster is very small; therefore, more space is required between fuel rods than between a rod and the channel wall.[10] Minor variations in the roughness of the outer channel wall do not seriously influence the flow distribution at the expected Reynolds number of about 50,000.

The stability of the fuel rods in the assembly is enhanced further by mid-length spacers. Both the end fixtures and the mid-length spacers disturb the flow so that the entire length of the rods is in a hydrodynamic entrance region. The

most recent correlation of air data[11] fits the data within +6% and -8%:

$$N_{Nu_b} = 0.041\ N_{Re_b}^{0.77}(L/D)^{-0.15},$$

where the temperature difference associated with the Nusselt number ($N_{Nu} = hD/k$) is based on the mixed mean gas temperature and the average surface temperature of the outer rods at a distance L from the nearest upstream spacer; the subscript b refers to mixed mean temperatures.

The rotational position of the assemblies in the coolant channel will be random. Thus, outer rods of a preceding assembly may partially block entrance to the spaces between the outer rods in the next assembly. The blockage will be most complete with a relative rotation of 30 degrees, while 60 degrees rotation is equivalent to no rotation. Apparently because of the mixing action of the spacers, a 30-degree rotation has little effect except just downstream from the spacers,but a 15-degree displacement of the preceding assembly produces a large eccentric variation in circumferential temperature along the entire first half of the rod and is easily detectable even beyond the mid-rod spacer. This effect results from a rotational flow component introduced by the unsymmetrical displacement of the preceding rods.

Pressure-drop measurements with atmospheric air[12] are well correlated over a range of Reynolds numbers by separating spacer and end effects from the remaining pressure drop. For the EGCR configuration $f = 0.17\ N_{Re_b}^{-0.18}$.

For spacers, the loss coefficients, defined as $c = 2\Delta p g_c/(\rho V^2)$, were largely independent of the main-stream Reynolds number, and were approximately 0.43 for the end supports for the rods and about 0.34 for the mid-rod spacers.

In calculating the local temperatures within the cluster, the following effects are considered: radial and axial heat-generation gradient, thermal radiation within the cluster, variable heat-transfer coefficient around the element and along the channel, gas temperature differences between the various flow passages, circumferential heat conduction around the graphite sleeve, and mixing between the flow passages. The flow of heat in the UO_2 pellets is assumed to be radial only. Analysis shows that at the end of the second assembly, where the heat generation is highest, the circumferential temperature difference between opposite sides of a fuel rod is 80° to 90°F.

4. The Peach Bottom HTGR Thermal Design

The Peach Bottom HTGR[13,2] is a helium-cooled reactor with semihomogeneous graphite fuel elements. The inlet temperature of 652°F lies above the level at which the Wigner effect in the graphite reflector is important, but still allows

the pressure vessel to be made of low-alloy steel. The outlet temperature of 1342°F is limited by the external circuits and not by the core.

The fuel element consists of a graphite spine of 1.75-in. diam, surrounded by a fuel ring of 2.75-in. diam that is contained in a graphite sleeve. The fuel ring consists of coated uranium and thorium carbide particles embedded in a graphite matrix. The elements form a closely packed hexagonal pattern with the 3.50-in. elements on a 3.55-in. pitch. Each element is surrounded by six tricuspid cooling passages. The elements are separated by four ring-shaped spacers.

A fuel ring was chosen rather than a solid central fuel cylinder of the same diameter to limit the peak temperature in the fuel; the present thickness of the ring is convenient for fabrication reasons. The sleeve is provided to keep fission products out of the primary coolant stream and to provide structural rigidity to the fuel element. Volatile fission products are purged from the element into fission-product traps.

The fuel element has no sharp temperature limitation (e.g., melting point, phase change) but fission-product release from the fuel particles increases appreciably between 2700° and 3000°F. The maximum design fuel temperature was taken to be 2700°F. A small local hot spot is not very serious, as a somewhat larger than normal fission-product release can be accepted in small areas of the core. It becomes more important, therefore, to know what percentage of the fuel is above certain temperatures rather than to try to prevent any fuel from reaching a limiting temperature.

The average heat-transfer coefficient and the circumferential variation of the heat-transfer coefficient around a fuel element were obtained experimentally.[14] Other uncertainties, such as the flow distribution in the reactor core and the effects of bending of fuel elements, were investigated analytically.

Experimental work[14] has shown that the smooth tube correlation using the hydraulic diameter of the tricuspid-shaped channel yields answers which are about 5% too high. The heat-transfer coefficient around the circumference varies between 55 and 130% of its average value. The friction factor for the channel lies slightly below the correlation for a smooth tube; however, the four spacers contribute approximately as much pressure drop as the channel friction.[15]

The following heat-transfer and friction-factor correlations are used in the design for Reynolds numbers between 15,000 and 100,000:

$$N_{Nu_f} = 0.021\, N_{Re_f}^{0.8}\, N_{Pr_f}^{0.4} \qquad \text{and} \qquad f = 0.079\, N_{Re_f}^{-0.25},$$

where the subscript f refers to properties evaluated at film temperature.

Temperature and pressure-drop calculations in the HTGR are complicated because the HTGR employs an open core, i.e., all cooling channels are interconnected and orificing is not possible. The local and total power input into the coolant varies from channel to channel; therefore, the resistance to flow also varies as a result of the differences in coolant viscosity and acceleration. The resulting pressure differences between channels are equalized by flow from one channel to another, i.e., cross-flow. At first sight, it is not obvious whether cross-flow is beneficial or disadvantageous: the hottest channel loses gas continuously because of higher accelerational and frictional local pressure drops, but more gas enters at the inlet of the hottest channel than would be possible for a closed hot channel. For the HTGR, it has been shown that these two effects approximately cancel each other, as far as maximum temperatures are concerned.

The change in coolant outlet temperature[2] in the HTGR resulting from sudden changes in power, coolant inlet temperature, or coolant flow rate is quite slow in comparison with other reactor systems because of the large heat capacity of the fuel element. HTGR transients are usually limited not by fuel-element temperatures but by the outlet temperatures that the ducts and steam generator can withstand. When coolant flow is interrupted, followed by a reactor scram, the fuel cools initially due to temperature equalization. The structural parts of ceramic elements (graphite) can withstand quite high temperatures without damage to the structural integrity of the element. In the Peach Bottom HTGR, emergency cooling is supplied by cooling the pressure vessel and transporting the afterheat from the fuel elements by conduction, natural convection, and radiation.

5. Pebble Bed Reactor Core Design

In selecting the core for a pebble bed reactor, assuming that the gas temperatures and total heat output are fixed, the relationship between the variables and the thermal-stress limitation places narrow limits on the range of values that one may select. In general, one wants the core power density large to minimize core dimensions, and the fuel elements large to minimize fuel fabrication cost and to simplify fuel handling. Typical core power densities are 5 to 10 kW/liter and ball diameters 1.5 to 2.5 in.

The importance of the core pressure drop depends on the direction of flow through the core. For a downward or radial-flow core, the restriction on pressure drop is the pumping power or structural-restraint limitations, whereas for an upward flow through the core, the limitation on pressure drop will be the levitation flow or flow rate at which the upper layer of fuel elements begins to move.

Experiments with gas flowing upward through beds of spheres have indicated that when the pressure gradient equals 80% of the bulk bed density, spinning of the balls in the upper layer begins;[16] at still higher flow rates, actual levitation of some spheres will occur. Recent studies have been summarized by Bundy.[17]

The relations used below are taken from Refs. [18] through [21]. Later data[22] indicate that the equation for pressure drop is not valid for $N_{Re} >$ 15,000. Above this value, the friction factor becomes a constant. The pressure drop through a bed of spheres may be expressed as

$$\Delta p = \frac{15\, G_s^{1.73}\, \mu^{0.27}\, L}{g_c\, \epsilon^3\, \rho[d/(1-\epsilon)]^{1.27}} ,$$

where G_s is the approach mass velocity, and d is the sphere diameter. The limit that thermal stress places on the mean power density in the ball bed is

$$q = 60(1-\nu)k\sigma_u(1-\epsilon)/(\alpha\, Ed^2\, \gamma) ,$$

where q is the maximum allowable mean power density, ν is Poisson's ratio, σ_u is the ultimate tensile strength, E is the modulus of elasticity, α is the coefficient of linear expansion, and γ is the maximum-to-mean power ratio.

The heat-transfer correlation for a bed of spheres is

$$N_{St} = 0.5\, N_{Pr}^{-0.66}\, [N_{Re}/(1-\epsilon)]^{-0.3} ,$$

with N_{St} and N_{Re} based on the superficial gas velocity and the ball diameter.

The mean surface-to-gas temperature drop is $\Delta t = qd/6h(1-\epsilon)$.

6. Surface Roughening and Swirl Flow

In gas-cooled reactors the film temperature drop is usually a larger fraction of the total temperature drop than in other types of reactors. It is therefore worthwhile to decrease the film temperature drop (Eq. 11). This may be accomplished in several ways: the heat-transfer surface FA may oe increased, the flow area ϵS may be decreased, and the Stanton number N_{St} may be increased. These three effects are compared in Ref. [23]. Many investigators, both in the United States and in other countries,[24-30] have studied experimentally and theoretically the ways of improving heat transfer with roughened surfaces. To obtain good performance, they found that the height of the turbulence promoters should be about the thickness of the laminar sublayer and the buffer layer. The friction factor becomes nearly independent of the Reynolds number, while the Stanton number decreases very slowly with increasing Reynolds number for turbulent flow of gases. For a given roughness height, there is an optimum ratio of pitch to height that produces the largest values of friction factor and Stantor number: ~7 to 8. The

best results given in Refs. [26] and [28] may be correlated by plotting the increase in Stanton number versus the increase in friction factor. Data from Refs. [24],[25] , and [29], among others, check with this correlation. The two following approximations seem to represent several sets of published data within ±10% for turbulent flow of gases such as air, nitrogen, CO_2, or helium, ($N_{Pr} \approx 0.7$), for $3 \times 10^4 < N_{Re} < 6 \times 10^5$, and for $1 \leq f^*/f \leq 3$:

$$N^*_{St}/N_{St} = (f^*/f)[1 + (f^*/f - 1)/4]^{-1}$$

$$f^*/f = (N^*_{St}/N_{St})^3 [1 + 5(N^*_{St}/N_{St} - 1)/3]^{-1} ,$$

where * refers to roughened surfaces. These equations show that doubling the Stanton number triples the friction factor. Surface roughening is currently used in the Windscale Advanced Gas Cooled Reactor and is now incorporated in the design of most advanced metal-clad gas-cooled reactors.

Swirl-flow heat transfer with gases in tubes has been studied with swirl induced by an internal twisted tape[31,32] and by tangential tube-wall slots.[33] The results show ratios of swirl-to-axial-flow heat-transfer coefficients at a given Reynolds number of 1.1 to 3.0 with increased friction factors. A good summary of data is given in Ref. [34].

7. Numerical Methods and Applications

Most of the thermal design analysis is performed by analysing a model by numerical methods. A number of digital computer codes have been developed in which thermal problems are solved by replacing the relevant differential equations by finite-difference equations. For coolant flow, one usually makes the approximation that the transit time of the gas through the coolant channel is small compared with the calculational time step. The finite-difference equations are often made implicit to avoid time-step limitations in transient problems. The solution of the simultaneous finite-difference equations is usually obtained by iterative methods as the number of unknown points is generally too large for effective matrix inversion and nonlinearities make it impractical in any case. Good, commonly used methods are the Peaceman-Rachford method for regular two-dimensional geometries or an extrapolated Liebman method for irregular or three-dimensional geometries. Nonlinearities (temperature-dependent properties, thermal radiation) are treated by re-evaluating the properties between iterations as a function of the current temperatures.

Codes for one-, two-, and three-dimensional geometries have been developed in which all thermal properties may be temperature-dependent, heat-generation rates

may be space- and time-dependent, radiation across internal gaps is permitted, and thermal expansion is taken into account. The boundary conditions may be completely general, e.g., radiation, conduction, and convection.

Such codes and also analytical methods have been applied to obtain temperature distributions in reactor cores and in complicated geometries such as those encountered in homogeneous fuel elements, e.g., fuel elements pierced by coolant channels, or fuel elements in which the fuel is concentrated in some regions of the element. With uniform convective cooling at the surface of circular equidistant cooling holes inside a circular cylinder, and with uniform heat generation, the optimum location of the holes is nearly independent of their dimension, for a given number of holes.[35] This optimum radial location is about 0.6 r for six holes or more, independent of the Biot number (N_{Bi} = hr/k). A similar problem is solved in Ref. [36] for a triangular or square cooling hole arrangement in a large solid with given coolant-hole surface temperature.

The fuel concentration in the annulus of an HTGR-type fuel element which gives the lowest internal hot spot and average temperature is found to be 50 to 65 volume-% for ratios of fuel-to-matrix thermal conductivities of 5 to 20%, respectively. This result is nearly independent of the total fraction of fuel in the element below about 25 volume-%; the thermal conductivity of fuel dispersed in the matrix may obey either a linear law or Maxwell's law.[37] For ratios of thermal conductivities above 45 to 50%, the annulus should contain fuel only, subject to metallurgical limitations.

The optimum shape of radial fuel holes in a spined cylindrical fuel element, cooled at the outside, has been studied as a function of various parameters, such as number of fuel holes of given total area, and ratio of conductivities of fuel to matrix.[38] The maximum internal fuel temperature is minimized with respect to the length-to-diameter ratio of the fuel holes. Circular holes are usually not as good as elongated pie-shaped holes for low fuel-to-matrix conductivity ratios.

Good neutron economy and high coolant temperatures can be obtained in all-ceramic (i.e., BeO) cores, but the heat flux for a given size fuel element is usually limited by tensile thermal stresses. Other coolants besides helium, e.g., CO_2, may be used at high temperatures in an all-BeO reactor. Steady-state temperatures and elastic thermal-stress distributions for several geometries with uniform internal heat generation have been tabulated.[39] It may be noted that the maximum tensile stress that occurs at the cooler boundary is proportional to the difference between average and surface fuel-element temperatures. Nonuniform internal heat generation has been studied extensively.[40] Elastic-plastic deformation of a

cylinder insulated on the outside and cooled inside, with uniform heat generation, has been studied.[41] The thermal-stress limitation for a given heat flux may be eased by cooling the ceramic fuel element both internally and externally. One can also use a graphite sleeve to provide structural strength to a BeO fuel element.[42]

Bounds for the efficiency of longitudinal fins of arbitrary shape with variable surface heat-transfer coefficient are given in Ref. [43]. The optimum shape of a fin with a given profile area and the corresponding maximum heat flux are quite different from the values obtained by using a constant heat-transfer coefficient.

In conclusion it may be stated that the design trend of gas-cooled power reactors in the U.S.A. has been towards high coolant outlet temperatures combined with simple (all-ceramic) fuel elements.

REFERENCES

1. Experimental Beryllium Oxide Reactor Program Quarterly Progress Report, USAEC Report GA-4386, General Atomic, July 31, 1963.
2. KATZ, R., and TROOST, M., Thermal Design Aspects of Gas-Cooled Reactors, USAEC Report GA-2944, General Atomic, 1962.
3. The 630-A Marine Reactor, Nucl. Eng., 9, 50-53 (February, 1964).
4. Army Reactor Systems Program, Power Reactor Technology, 6, No. 3, 57-60 (June, 1963).
5. Ultra High Temperature Reactor Experiment (UHTREX), Hazard Report, USAEC Report LA-2689, Los Alamos Scientific Laboratory, April 20, 1962.
6. SAMUELS, G., Design and Analysis of the Experimental Gas-Cooled Reactor Fuel Assemblies, USAEC Report ORNL-3478, Oak Ridge National Laboratory, September 27, 1963.
7. CRANDALL, W. H., and HIGGINS, R. M., Pressure Drop Experiments of the Title II Fuel Assembly for the Experimental Gas-Cooled Reactor, Section III of the Fuel Assembly Heat Transfer and Channel Pressure Drop Experiments for the EGCR Research and Development Program, USAEC Report RD-0009, Allis-Chalmers Mfg. Company, October 3, 1960.
8. Heat Transfer Experiments of the Title II Fuel Assembly for the Experimental Gas-Cooled Reactor, USAEC Report RD-0010, Allis-Chalmers Mfg. Company.
9. WANTLAND, J. L., and MILLER, R. L., Heat Transfer in Septafoil Geometries by Mass-Transfer Measurements, USAEC Report CF-59-6-9, Oak Ridge National Laboratory, June 30, 1959.
10. Gas Cooled Reactor Project Quarterly Progress Reports, USAEC Reports ORNL-2964, June 30, 1960, ORNL-3015, September 30, 1960, ORNL-3049, December 31, 1960, Oak Ridge National Laboratory, 1960.
11. KIDD, G. J., Experimental Determination of the Temperature Structure and Heat-Transfer Characteristics of the EGCR Title II Fuel-Element Assembly, USAEC Report ORNL-TM-807, Oak Ridge National Laboratory, to be published.

12. KIDD, G. J., and WANTLAND, J. L., Pressure Drop Characteristics of Circular Ducts Containing Septafoil Rod Clusters, USAEC Report ORNL-TM-703, Oak Ridge National Laboratory, October 15, 1963.

13. FORTESCUE, P., NICOLL, D., RICKARD, C., and ROSE, D., HTGR —Underlying Principles and Design, Nucleonics, 18, No. 1, 86-90 (1960).

14. PALMER, L. D., and SWANSON, L. L., Measurements of Heat-Transfer Coefficients, Friction Factors, and Velocity Profiles for Air Flowing Parallel to Closely Spaced Rods, Proc. International Heat Transfer Conference, August, 1961, Part III, pp. 535-542, The American Society of Mechanical Engineers, New York, N.Y., 1961.

15. ROSS, S., DAY, E. A., and SKEEHAN, R. A., Tests on Half-Scale Model of 40-MW(e) Prototype HTGR, USAEC Report GA-2963, General Atomic, June 20, 1962.

16. BUNDY, R. D., Full-Scale Packed-Bed Reactor Core Experiments, Gas Cooled Reactor Program Semiannual Progress Report, Period ending March 31, 1962, USAEC Report ORNL-3445, Oak Ridge National Laboratory, 1962, pp. 308-325.

17. BUNDY, R. D., Summary of Recent Literature with Application to Pebble Bed Reactors, Report ORNL-TM-806, Oak Ridge National Laboratory, to be published.

18. Design and Feasibility of a Pebble Bed Reactor Steam Plant, USAEC Report NYO-8573, Sanderson and Porter, 1958.

19. FRAAS, A. P., CARLSMITH, R. S., CORAN, J. M., et al., Preliminary Design of a 10-MW(t) Pebble-Bed Reactor Experiment, USAEC Report ORNL-CF-60-10-63 (rev.), Oak Ridge National Laboratory, May 8, 1961.

20. FRAAS, A. P., CARLSMITH, R. S., CORAN, J. M. et al., Design Study of a Pebble-Bed Reactor Power Plant, USAEC Report ORNL-CF-60-12-5 (rev.), Oak Ridge National Laboratory, May 11, 1961.

21. Conceptual Design of the Pebble Bed Reactor Experiment, USAEC Report ORNL-TM-201, Oak Ridge National Laboratory, May 17, 1962.

22. TOUCHTON, W. F., Jr., Pressure Drops Through Cylindrical Beds of Packed Spheres, Franklin Institute Report F-B 1994, February, 1963.

23. MELESE, G. B., Comparison of Partial Roughening of the Surface of Fuel Elements with Other Ways of Improving Thermal Performance of a Nuclear Reactor, Trans. Am. Nucl. Soc., 6 (November, 1963), pp. 337-338.

24. KEMENY, G. A., and CYPHERS, J. A., Heat Transfer and Pressure Drop in an Annular Gap with Surface Spoilers, J. Heat Transfer, 83 (1961) pp. 189-198.

25. DIPPREY, D. F., and SABERSKY, R. H., Heat and Momentum Transfer in Smooth and Rough Tubes at Various Prandtl Numbers, Inter. J. Heat Mass Transfer, 6 (1963), pp. 329-353.

26. KATTCHEE, N., and MACKEWICZ, W. V., Heat-Transfer and Fluid Friction Characteristics of Tube Clusters with Boundary-Layer Turbulence Promoters, ASME Paper No. 63-HT-1, 1963.

27. KATTCHEE, N., and MACKEWICZ, W. V., Effects of Boundary Layer Turbulence Promoters on the Local Film Coefficients of ML-1 Fuel Elements, Nuclear Sci. and Eng., 16, No. 1 (1963), pp. 31-38.

28. WALKER, V., and RAPIER, A. C., Fuel Element Heat Transfer, J. Brit. Nuclear Energy Soc., 2 (April, 1963), pp. 268-275.

29. NUNNER, W., Heat Transfer and Pressure Drop in Rough Tubes, VDI Forschungheft 455, Series B, 22, 5 - 39 (1956). AERE Lib/Trans. 786, 1958.

30. MALHERBE, J. M., Influence des rugosités de paroi sur les coefficients d'échange thermique et de perte de charge, CEA-2283, 1963.

31. KREITH, F., and MARGOLIS, D., Heat Transfer and Friction in Turbulent Vortex Flow, Appl. Sci. Res., Sec. A, 8, 457-473 (1959).

32. SMITHBERG, E., and LANDIS, F., Friction and Forced Convection Heat-Transfer Characteristics in Tubes with Twisted Tape Swirl Generators, ASME Paper No. 62-WA-176, 1962.

33. GREEN, N. D., and GAMBILL, W. R., A Preliminary Investigation of Air Film Heat-Transfer Coefficients for Free- and Forced-Vortex Flows Within Tubes, USAEC Report CF-58-5-67, Oak Ridge National Laboratory, May 23, 1958.

34. GAMBILL, W. R., and BUNDY, R. D., An Evaluation of the Present Status of Swirl-Flow Heat Transfer, ASME Paper No. 62-HT-42, 1962: also USAEC Report CF-61-4-61, Oak Ridge National Laboratory, April 24, 1961.

35. ROWLEY, J. C., and PAYNE, J. B., Steady State Temperature Solution for a Heat-Generating Circular Cylinder Cooled by a Ring of Holes, J. Heat Transfer, Trans. ASME (1964).

36. SPARROW, E. M., Temperature Distribution in an Internally Cooled, Heat-Generating Solid, ASME Paper 60-SA-15, 1960.

37. Advanced Beryllium Oxide Concepts, Progress Report for the Period Ending March 31, 1964, USAEC Report GA-5036, General Atomic, to be published.

38. Advanced Beryllium Oxide Concepts, Progress Report for the Period Ending December 31, 1963, USAEC Report GA-4966, General Atomic.

39. HANKEL, Ralph, Stress and Temperature Distribution, Nucleonics, 18 (November, 1960), 168-169.

40. MELESE, G. B., and WILKINS, J. E., Jr., Heat Conduction in a One Dimensional Geometry with Nonuniform Internal Heat Generation, Trans. Am. Nuclear Soc., 5, No. 1 (June, 1962), pp. 142-143.

41. BEYER, W. A., An Elastic-Plastic Cylinder with Free Ends and Internal Heat Generation, Nuclear Sci. and Eng., 17 (October, 1963), pp. 179-184.

42. MC WHIRTER, A. D., and GOODJOHN, A. J., Beryllium Oxide as a Moderator in High-Temperature, Gas-Cooled Reactors, Trans. Am. Nuclear Soc., 6, No. 2, (1963), p. 330.

43. MELESE, G. B., and WILKINS, E. J., Jr., On the Efficiency of Longitudinal Fins of Arbitrary Shape with Variable Surface Heat Transfer Coefficient, Report GA-4559, General Atomic, 1963.

Table I

THERMAL CHARACTERISTICS OF SOME U.S. GAS-COOLED REACTORS

	EGCR	HTGR	EBOR	630-A	ML-1	UHTREX
Power						
Thermal, MW(th)	85	115.5	10	67.4	3.3	3
Electrical, MW(e)	25	40	None	20	0.33	None
Active core						
Diameter, m	3.6	2.8	0.59 side	1.22	0.56	0.585 I.D. 1.78 O.D.
Length, m	4.4	2.3	1.93	0.70	0.56	1.0
Power density, kW/liter of core	1.87	8.3	13.7	82.5	15.3	1.3
Power conversion	482°C steam 87 atm	537°C steam 95 atm	None	510°C steam 60 atm	Closed-cycle gas turbine	None
Heat flux						
W/cm^2	55 (max)	35 (max)	84 (max)	19 (avg)	44.5 (max)	35 (max)
W/cm	330 (max)	980 (max)	251 (max)	1000 (avg)	85 (max)	140 (max)
Maximum temperature, °C						
Surface	816	1050	815	----	955	1593
Fuel	1650	1330	1040	813	1180(UO_2-BeO) 1450(UO_2)	1610
Coolant gas	Helium	Helium	Helium	Air	N_2 or Air	Helium
Total mass flow, kg/sec	53.5	55.5	6.3	160	11.3	1.29
Inlet temperature, °C	266	345	400	300	422	870
Outlet temperature, °C	566	728	700	650	650	1320
Pressure, atm	22	23.0	72.5	27	20.5	34
Coolant void fraction, %	6.2	12.8	11	----	----	----
Reactor pumping fraction, %	2	0.55	1.4	3[a]	3.3[a]	0.07
Moderator	C	C (in element)	BeO	Water	Water	C
Number of channels	234	804 elements	36	85[b]	61[b]	312[c]
Fuel	UO_2	UC_2, ThC_2 in C	UO_2-BeO	UO_2[d]	UO_2, UO_2-BeO	UO_2 in C
Enrichment, %	2.46	93.5	62.5	93.5	93.5	93.5
Cladding material	304 SS	C	Hastelloy-X	80Ni-20Cr	Hastelloy-X	None
Cladding thickness, cm	0.05	0.95	0.05	0.10	0.075	----
Fuel region I.D. and O.D., cm	0.82×1.8[e]	1.45×7.0	0.0×0.85[f]	0.45[g]	0.0×0.46[h]	1.27×2.54
Fuel-element length, cm	6×73.6	366	210	9×7.65	79	4×14

[a] Primary loop.
[b] Pressure tubes.
[c] 13 levels of 24 radial channels.
[d] 38.2 wt-% UO_2 in 80 Ni-20Cr alloy.
[e] An element contains 7 pins.
[f] An element consists of an annular ring of 18 rods around a BeO spine.
[g] 10-13 concentric rings 0.45-cm thick, cooled on both sides.
[h] An element contains 19 pins (18 fueled).

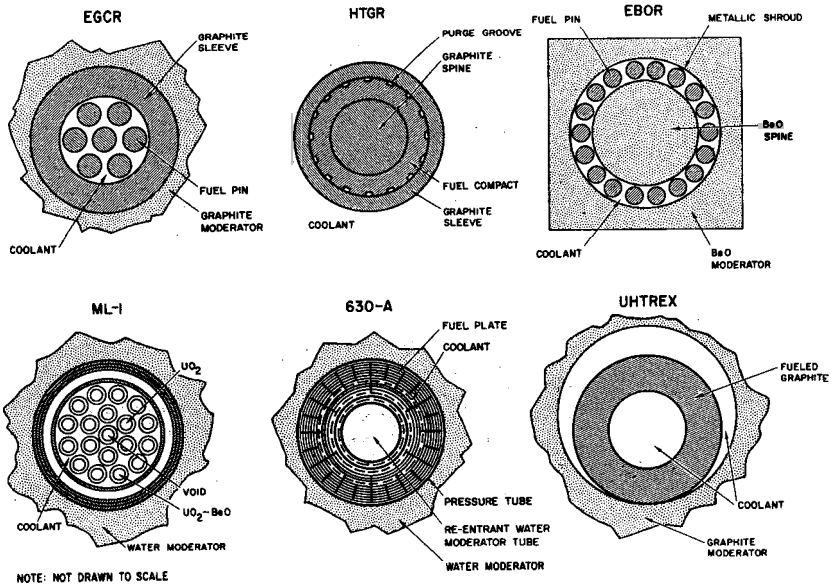

Fig. 1. Schematic fuel-element cross sections for the reactors of Table I

THERMAL DESIGN ASPECTS OF GAS-COOLED POWER REACTOR CORES

by

M. Troost
P. Fortescue
R. N. Lyon
G. Melese
G. Samuels

List of Figures